



# Efficiency of regional functional liver volume assessment using Gd-EOB-DTPA-enhanced magnetic resonance imaging for hepatocellular carcinoma with portal vein tumor thrombus

Kenichiro Araki<sup>1</sup> · Norifumi Harimoto<sup>1</sup> · Takahiro Yamanaka<sup>1</sup> · Norihiro Ishii<sup>1</sup> · Mariko Tsukagoshi<sup>1</sup> · Takamichi Igarashi<sup>1</sup> · Akira Watanabe<sup>1</sup> · Norio Kubo<sup>1</sup> · Yoshito Tsushima<sup>2</sup> · Ken Shirabe<sup>1</sup>

Received: 4 February 2020 / Accepted: 17 May 2020 / Published online: 1 July 2020  
© Springer Nature Singapore Pte Ltd. 2020

## Abstract

**Purpose** We investigated whether functional future remnant liver volume (fFRLV), assessed using gadolinium-ethoxybenzyl-diethylenetriamine pentaacetic acid-enhanced magnetic resonance imaging (EOB-MRI), could evaluate regional liver function in hepatocellular carcinoma (HCC) patients with portal vein tumor thrombus (PVTT) and help establish the indication for hepatectomy.

**Methods** The subjects of this study were 12 patients with PVTT [PVTT(+) group] and 58 patients without PVTT [PVTT(−) group], from among 191 patients who underwent hepatectomy of more than one segment for HCC. We calculated the liver-to-muscle ratio (LMR) in the remnant liver, using EOB-MRI and fFRLV. Preoperative factors and surgical outcome were compared between the groups. The LMR of the area occluded by PVTT was compared with that of the non-occluded area.

**Results** The indocyanine green retention rate at 15 min (ICG-R15) and liver fibrosis indices were increased in the PVTT(+) group, but the surgical outcomes of patients in this group were acceptable, with no liver failure, no mortality, and no differences from those in the PVTT(−) group. The fFRLV in the PVTT(+) group was not significantly different from that in the PVTT(−) group ( $p=0.663$ ). The LMR was significantly lower in the occluded area than in the non-occluded area ( $p=0.004$ ), indicating decreased liver function.

**Conclusion** Assessing fFRLV using EOB-MRI could be useful for evaluating regional liver function and establishing operative indications for HCC with PVTT.

**Keywords** EOB-MRI · Functional liver volume · Portal vein tumor thrombus · Regional liver functional reserve

**Electronic supplementary material** The online version of this article (<https://doi.org/10.1007/s00595-020-02062-y>) contains supplementary material, which is available to authorized users.

✉ Norifumi Harimoto  
nharimotoh1@gmail.com

<sup>1</sup> Division of Hepatobiliary and Pancreatic Surgery,  
Department of General Surgical Science, Gunma University  
Graduate School of Medicine, 3-39-22 Showa-machi,  
Maebashi, Gunma 371-8511, Japan

<sup>2</sup> Department of Diagnostic Radiology and Nuclear Medicine,  
Gunma University Graduate School of Medicine, Gunma,  
Japan

## Introduction

Vascular invasion is an important prognostic factor in patients with hepatocellular carcinoma (HCC), which tends to spread through the portal veins [1]. The median survival of untreated patients with portal vein tumor thrombus (PVTT) has been reported as only 2.7 months, and even those who received effective treatment have survived for a median of just 6.4–20.0 months [2–6]. Hepatic resection could be an effective option, as part of multidisciplinary treatment, even for advanced HCC. Some reports have demonstrated that surgical treatment is feasible for selected HCC patients with PVTT with a resectable tumor and moderate liver function, to prolong survival and improve quality of life. However, this is only if PVTT is limited to the first-order branch, whereas non-surgical treatments fail to provide comparable therapeutic effects [7]. Occlusion by

PVTT deteriorates liver function, and background liver diseases, such as viral infection or fatty liver, can exclude hepatic resection as a surgical option. The liver area including occlusion by PVTT is expected to have less functional reserve than the non-occluded area. Therefore, it is important to evaluate and compare the “regional” functional reserve between the occluded area and the non-occluded area precisely.

Contrast agents, such as gadolinium-ethoxybenzyl-diethylenetriamine pentaacetic acid (Gd-EOB-DTPA), are specifically taken up by hepatocytes. Therefore, Gd-EOB-DTPA-enhanced MRI (EOB-MRI) can reflect the liver functional reserve. Several recent reports have shown that EOB-MRI is useful for the quantitative evaluation of liver function [8–10]. Previously, we reported the usefulness of assessing functional future remnant liver volume (fFRLV) preoperatively, using EOB-MRI to predict postoperative liver-related complications in patients undergoing HCC resection [11]. We also reported that fFRLV assessed using EOB-MRI could predict post-hepatectomy liver failure (PHLF) precisely in patients undergoing resection of more than one segment [12]. As fFRLV assessment using EOB-MRI has the advantage of being a regional functional assessment, unlike other examinations that assess the whole-liver function, it could be useful for evaluating future remnant liver function in areas not occluded by PVTT. We conducted this study to evaluate the efficiency of FRLV assessment using EOB-MRI in HCC patients with or without PVTT, and investigate the surgical outcomes of those patients for a precise indication of hepatectomy.

## Methods

### Patient population

We collected data retrospectively on 191 patients who underwent hepatectomy for HCC resection between January, 2009 and October, 2019 in the Division of Hepatobiliary and Pancreatic Surgery of our hospital. Patients who did not undergo preoperative EOB-MRI were excluded. In this series, there were 12 patients with PVTT, diagnosed either as Vp2 (second-order branches), Vp3 (first-order branches), or Vp4 (portal trunk) according to the General Rules for Clinical and Pathological Study of Primary Liver Cancer in Japan. Seventy of the 191 patients underwent hepatectomy of more than one segment and these patients were divided into two groups for comparative analysis: those with [PVTT(+)] group,  $n = 12$ ] and those without PVTT [PVTT(-)] group,  $n = 58$ ].

The clinical and perioperative data analyzed in this patient series included sex, age, liver function indicators [platelet count, prothrombin time (PT), total bilirubin,

alanine transaminase, and albumin], fibrosis markers [hyaluronic acid, type 4 collagen, and Mac-2 binding protein glycan isomer (M2BPGi)], indocyanine green retention rate at 15 min (ICG-R15), liver stiffness measured using Virtual Touch Quantification (VTQ) imaging, preoperative computed tomography (CT) findings, type of hepatectomy, remnant liver volume (RLV), and RLV rate. The plasma disappearance rate of the ICG (ICG-K) value was also calculated from the ICG-R15 value and used as a total liver function test.

Postoperative complications were categorized on the basis of Clavien–Dindo classification [13]. Postoperative severe complications were defined as grade III or more. PHLF was diagnosed according to the International Study Group of Liver Surgery definition [14]; namely, an elevated PT-international normalized ratio and concomitant hyperbilirubinemia on or after postoperative day 5), and PHLF was defined as grade B or C. We assessed surgical outcomes in all patients using fFRLV values. The study protocol was approved by our institutional ethics committee (approval no. 1597, HS2019-066).

### Imaging of regional liver functional reserve using EOB-MRI and functional liver volume assessment

The methodology of regional liver functional reserve assessment using EOB-MRI and that of functional liver volume assessment have been described previously [12]. First, preoperative contrast-enhanced multidetector CT images were reconstructed into three-dimensional (3D) images using a SYNAPSE VINCENT volume analyzer system (FUJIFILM Co., Tokyo, Japan) from the Digital Imaging and Communications in Medicine (DICOM) data. The total liver volume, future remnant liver volume (FRLV) after hepatectomy, and percentage of RLV (%RLV) were calculated, and vascular mapping was performed using this system.

EOB-MRI was performed using a MAGNETOM Skyra 3T or Prisma 3T scanner (Siemens Healthcare K.K., Tokyo, Japan). A multiphase dynamic study, including arterial, portal, and late phases, was performed using axial 3D volume interpolated breath-hold examination after the intravenous injection of 0.1 mL/kg EOB-Primovist (Bayer Yakuin Ltd., Osaka, Japan). T1-weighted images (retention time 3.0 ms, echo time 1.05 ms, slice thickness 2.5 mm) of the pre-enhanced and hepatobiliary phases, obtained 20 min after the injection of EOB-Primovist, were used for image assessments [8, 15, 16].

The signal intensity (SI) of the remnant liver was measured on the DICOM viewer (NEOVISTA I-PACS VR; Konica Minolta Inc., Tokyo, Japan) by selecting a region of interest in the remnant liver, avoiding vessels and artifacts. The SI of the spinal column erector muscle was also calculated for standardization of the SI value in each patient. After calculating the

average of 10 fields of SI in both the remnant liver and muscle, the liver-to-muscle ratio (LMR) was derived by dividing the average SI of the remnant liver by the average SI of muscle (Fig. 1a). Finally, fFRLV ( $\text{mL}/\text{m}^2$ ) was calculated by multiplying LMR and remnant volume, and standardized by dividing by the body surface area ( $\text{m}^2$ ), as follows:

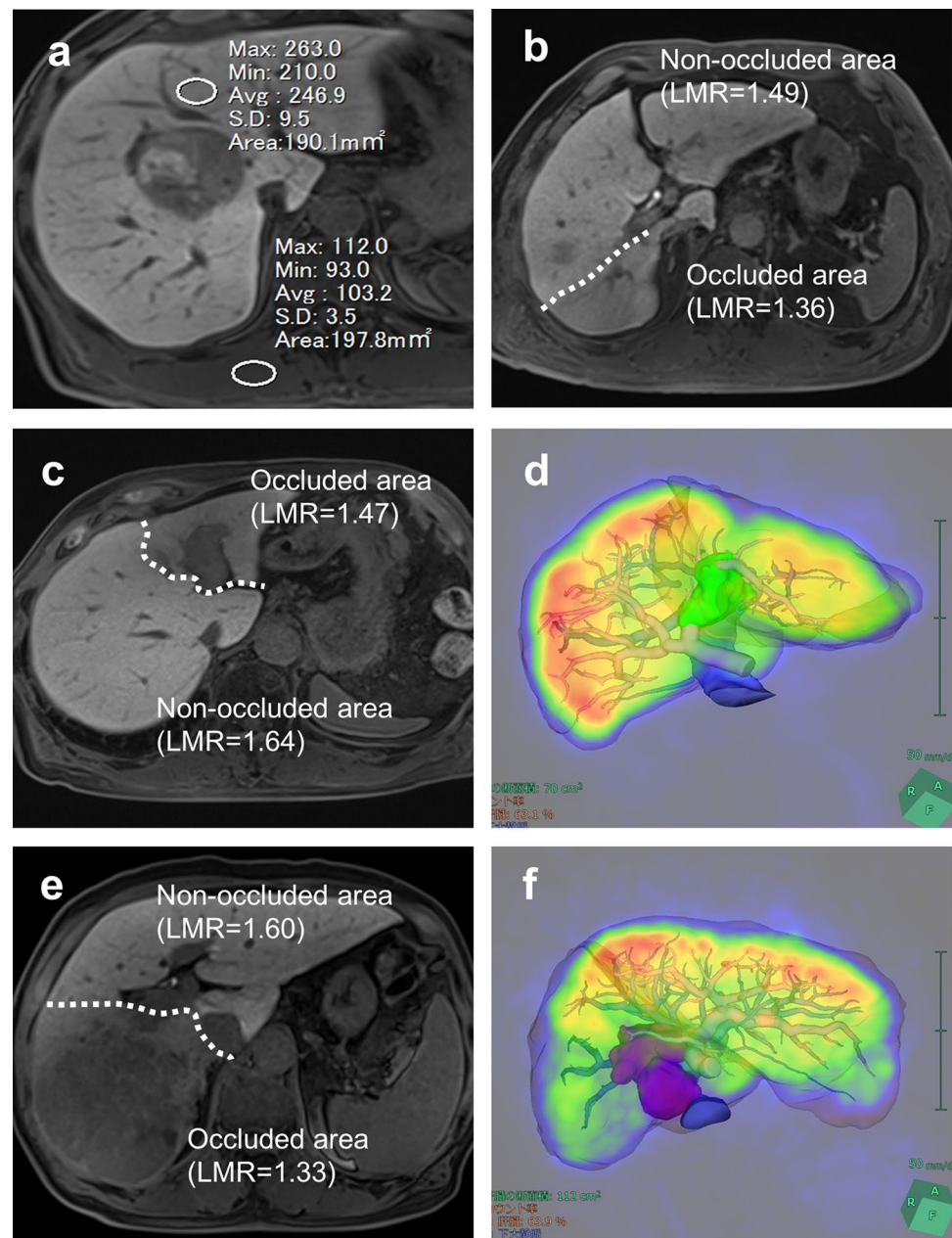
$$\text{LMR} = \frac{\frac{\text{Average SI after 20 min of injection (remnant liver)}}{\text{Average SI before injection (remnant liver)}}}{\frac{\text{Average SI after 20 min of injection (muscle)}}{\text{Average SI before injection (muscle)}}}$$

$$\text{fFRLV}(\text{mL}/\text{m}^2) = \frac{\text{LMR} \times \text{Remnant liver volume (ml)}}{\text{Body Surface area (m}^2\text{)}}$$

### Analysis with other functional remnant liver assessments using ICG-Krem values and 3D-CT/Tc-GSA single photon emission computed tomography (SPECT) fusion imaging

A previous report indicated that ICG-K and %RLV predict the PHLF and postoperative mortality of patients who have undergone PVE [17]. We calculated the ICG-K of the remnant liver volume (ICG-Krem) using the formula:

**Fig. 1** **a** Measurement of signal intensity in the region of interest on the T1-weighted image (T1WI) of the enhanced phase (T1WI) of the enhanced phase 20 min after gadolinium-ethoxybenzyl-diethylenetriamine pentaacetic acid injection. **b** T1WI of the enhanced phase (20 min) in patient No. 6. The signal intensity and liver-to-muscle ratio (LMR) of the area occluded by portal vein tumor thrombus (PVTT) area tended to be lower than those of the non-occluded area. This patient had occlusion of the posterior portal branch by PVTT. The dotted line indicates the boundary between the occluded area and the non-occluded area. **c** T1WI of the enhanced phase (20 min) in an HCC patient with PVTT (No. 5). This patient also had an occlusion of the left portal branch by PVTT. The dotted line indicates the boundary between the occluded area and the non-occluded area. **d** The image of the 3D-CT/SPECT fusion method in patient No. 5. The area occluded by PVTT showed relatively low accumulation of Tc-GSA. **e** T1WI of the enhanced phase (20 min) in patient No. 12. This patient had occlusion of the right portal branch by PVTT. The dotted line indicates the boundary between the occluded area and the non-occluded area. **f** The image of 3D-CT/SPECT fusion method in patient No. 12. The area occluded by PVTT showed relatively low accumulation of Tc-GSA



ICG-K  $\times$  %RLV (%) / 100. We then compared the surgical outcomes between fFRLV using EOB-MRI and ICG-Krem in the PVTT(+) group.

Preoperative  $^{99m}\text{Tc}$ -GSA scintigraphy was performed separately from CT. Dynamic scanning was initially performed using a large-field view gamma camera (E.CAM; Toshiba Japan, Tokyo) in an anterior view equipped with a low-energy high-resolution collimator, with the patient in the supine position after a bolus intravenous injection of 185 MBq of  $^{99m}\text{Tc}$ -GSA. Dynamic planar images were obtained for 20 min using 15 s  $\times$  80 frames, with a matrix size of 128  $\times$  128. Hepatic SPECT images were acquired after the dynamic study. The DICOM data obtained from SPECT were also imported to a SYNAPSE VINCENT system and subsequently fused with the 3D-CT images (Fig. 1d, f). The functional %RLV using 3D-CT/SPECT fusion were automatically calculated using the SYNAPSE VINCENT system. We compared the surgical outcomes between fFRLV using EOB-MRI and %RLV using 3D-CT/SPECT fusion in the PVTT(+) group.

### Preoperative assessment for operative indication and surgical procedure

In this series, the indication for hepatectomy was established using future liver remnant volume [18], as well as the platelet count, PT, albumin, total bilirubin, ICG-R15, and liver fibrosis markers.

Our surgical procedures for liver resection are described briefly as follows: Liver parenchymal transection was performed primarily with a Cavitron Ultrasonic Surgical Aspirator (AMCO Inc., Tokyo, Japan). Hemostasis was achieved using a monopolar coagulating device (IO-electrode; AMCO Inc., Tokyo, Japan) connected to a VIO300D generator (ERBE GmbH, Germany), used in soft coagulation mode. An intermittent pedicle clamp (15 min occlusion and 5 min reperfusion) was used routinely with parenchymal transection. Hemodynamic management under anesthesia was applied to maintain low central vena caval pressure to minimize blood loss with reduced perfusion [19, 20]. If necessary, the infrahepatic inferior vena cava was encircled and partially clamped to reduce perfusion [19, 21, 22].

### Statistical analysis

Continuous data are presented as means  $\pm$  standard deviation (SD) and as the median (range) for variables with normal and non-normal distribution, respectively. Differences between the two cohorts were assessed using Fisher's exact test and the Mann–Whitney *U* test, as appropriate. Correlations between ICG-R15 and LMR (or fFRLV) and those between fFRLV and ICG-Krem (or functional %RLV of 3D-CT/SPECT fusion) were assessed using Pearson's

correlation coefficients. All statistical analyses were performed using SPSS Statistics software version 24.0 (IBM SPSS Inc., Chicago, IL).  $P < 0.05$  was considered significant.

## Results

### Characteristics of HCC patients with and without PVTT

Table 1 summarizes the characteristics of the HCC patients with PVTT ( $n = 12$ ;  $\geq Vp2$ ) vs. those without PVTT ( $n = 58$ ;  $< Vp2$ ), who underwent hepatectomy of more than one segment. There were no differences in liver background diseases, values of liver function parameters, or levels of tumor markers between the two groups. According to the results of fibrosis makers and liver stiffness indices, M2BPGi ( $p = 0.008$ ) and VTQ ( $p = 0.013$ ) were significantly worse in the PVTT(+) group, but hyaluronic acid and type 4 collagen were not ( $p = 0.062$  and  $0.380$ , respectively). ICG-R15 was significantly higher in the PVTT(+) group than in the PVTT(−) group (median 20.9% vs. 13.5%,  $p = 0.009$ ). Imaging analysis revealed that future RLV, future remnant volume rate, and fFRLV were not different in the two groups ( $p = 0.094$ ,  $0.130$ , and  $0.663$ , respectively). In contrast, LMR was higher in the PVTT(−) group ( $p = 0.050$ ).

Operation times and blood loss were similar in the two groups ( $p = 0.212$  and  $0.407$ , respectively), as was the rate of intraoperative blood transfusion ( $p = 0.121$ ). Postoperative major complications, defined as Clavien–Dindo classification grade III or higher, tended to be more frequent in the PVTT(+) group, but the difference was not significant (25.0% vs. 13.8%,  $p = 0.061$ ). PHLF occurred in three patients (5.2%) from the PVTT(−) group and in none from the PVTT(+) group. Two patients underwent right hepatectomy. One suffered severe intraoperative bleeding (4120 mL) and PHLF, which improved with conservative treatment including plasma transfusion. The other patient was an 80-year-old man with sarcopenia; hence, we administered preoperative nutritional support and physical rehabilitation, but postoperatively he had PHLF, pneumonia, and disuse syndrome. This patient had been treated and was transferred to another hospital on postoperative day 196. Another patient underwent a right tri-sectionectomy and suffered severe intraoperative bleeding (9625 mL) and PHLF. The PHLF improved with conservative treatment including plasma transfusion, and he was discharged on postoperative day 74.

There was no mortality in this series and the length of the hospital stay after surgery was similar in the two groups ( $p = 0.369$ ). The fFRLV values were compared between the two groups, including the occurrence of PHLF. Figure 2 shows each fFRLV value in the two groups and the

**Table 1** Characteristics of the hepatocellular carcinoma patients without vs. those with portal vein tumor thrombus

	PVTT(-): < Vp2 (n = 58)	PVTT(+): ≥ Vp2 (n = 12)	p value
General background			
Age (years)	69 ± 9	70 ± 5	0.704
Sex			
Male	48	10	0.141
Female	11	2	
BMI (kg/m <sup>2</sup> )	23.3 ± 3.2	23.1 ± 3.9	0.998
Background liver diseases			
HBV	5	1	0.658
HCV	25	6	
Others	28	5	
Blood examination			
Platelet count (×10 <sup>3</sup> /μL)	183 ± 66	173 ± 62	0.663
PT (%)	97 ± 11	97 ± 9	0.751
Alanine transaminase (IU/L)	48 ± 64	45 ± 33	0.745
Total bilirubin (mg/dL)	0.8 ± 0.4	0.7 ± 0.2	0.438
Albumin (g/dL)	3.9 ± 0.6	3.9 ± 0.4	0.340
Fibrosis markers and indicators			
Hyaluronic acid (ng/mL)	97 ± 90	153 ± 87	0.076
Type 4 collagen	184 ± 69	210 ± 57	0.142
M2BPGi (COI)	1.00 (0.31–4.66)	2.07 (0.97–5.62)	0.008
Liver stiffness measurement			
VTQ (m/s)	1.29 (0.88–3.11)	2.10 (1.01–3.15)	0.013
Indocyanine green test			
ICG-R15 (%)	13.5 (3.4–33.2)	20.9 (8.6–36.2)	0.009
Tumor markers			
AFP (ng/mL)	42 (2–36,843)	31 (3–8108)	0.764
DCP (mAU/m)	57 (12–96,380)	341 (18–24,077)	0.624
Tumor size (cm)	6.1 (1.4–12.5)	6.1 (1.3–11.7)	0.913
Image analysis			
FRLV (mL)	738 (338–1495)	883 (531–1281)	0.094
%RLV (%)	63.7 (31.8–88.9)	67.8 (44.2–79.1)	0.130
LMR	1.69 (0.83–2.40)	1.55 (1.13–1.82)	0.050
fFRLV (mL/m <sup>2</sup> )	802 (292–1486)	800 (486–1242)	0.663
Surgical outcomes			
Operation time (min)	396 (244–712)	470 (320–682)	0.212
Blood loss (mL)	413 (35–9625)	339 (61–2368)	0.407
Intraoperative blood transfusion	9 (15.5%)	2 (16.7%)	0.121
Postoperative course			
Major complication, ≥ C-D grade III	8 (13.8%)	3 (25%)	0.061
PHLF	3 (5.2%)	0	0.616
Mortality	0	0	–
Length of hospital stay	14 (9–196)	18 (10–37)	0.369

HCC hepatocellular carcinoma, PVTT portal vein tumor thrombus, BMI body mass index, HBV hepatitis B virus, HCV hepatitis C virus, PT prothrombin time, M2BPGi Mac-2 binding protein glycan isomer, COI cutoff index, VTQ Virtual Touch Quantification, ICG-R15 indocyanine green retention rate at 15 min, AFP alpha-fetoprotein, DCP des-gamma-carboxy prothrombin, FRLV future remnant liver volume, %RLV percentage of FRLV, fFRLV functional future remnant liver volume, C-D Clavien–Dindo classification, PHLF post-hepatectomy liver failure

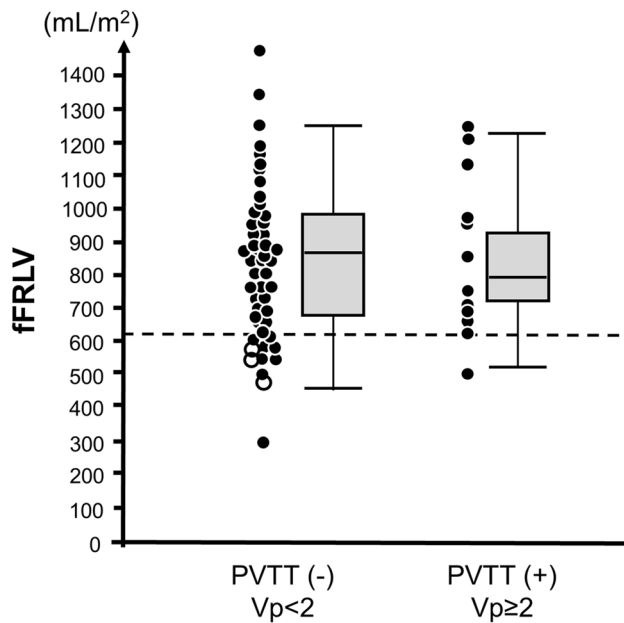


**Fig. 2** Relationships between functional future remnant liver volume (fFRLV) values in the portal vein tumor thrombus-negative [PVTT(-)] group ( $n=58$ ) and the PVTT(+) group ( $n=12$ ). The dotted line indicates the cutoff value of fFRLV ( $615 \text{ mL/m}^2$ ) for predicting post-hepatectomy liver failure (PHLF) [12]. White circles indicate patients with PHLF ( $n=3$ ) in the PVTT(-) group

relationship to the cutoff value ( $615 \text{ mL/m}^2$ ) for predicting PHLF. All three patients with PHLF in the PVTT(-) group had an fFRLV below the cutoff value (Fig. 2).

### Characteristics of the HCC patients with PVTT

Table 2 summarizes the characteristics of the 12 HCC patients with PVTT (10 men, 2 women; mean age,  $70 \pm 5$  years). The underlying liver diseases were hepatitis C virus infection in six patients, hepatitis B virus infection in one patient, and non-B non-C liver dysfunction of other causes in five patients. PVTT invaded the main portal trunk in two patients (Vp4), the primary portal branch in six patients (Vp3, left in five patients and right in one patient), and the second branch in four patients (Vp2, left lateral portal branch in two patients and right posterior portal branch in two patients). The median tumor diameter was 7.2 cm (range 1.3–11.7 cm). The median fFRLV was  $800 \text{ mL/m}^2$  (range 486–1242  $\text{mL/m}^2$ ), and the median ICG-R15 was 20.9% (range 8.6–36.2%).

### Surgical outcomes of HCC patients with PVTT

Table 3 shows the surgical outcomes in the PVTT(+) group. The type of hepatectomy was left hepatectomy including extended left hepatectomy in eight patients, right

hepatectomy including extended right hepatectomy in three patients, and posterior sectionectomy in one patient. The median operative time was 470 min (range 320–682 min), with a median blood loss of 339 mL (range 61–2368 mL). Intraoperative blood transfusion was performed in two patients. One patient (No. 5) had severe blood loss (2368 mL), and the fFRLV ( $486 \text{ mL/m}^2$ ) of this patient was below the cutoff value ( $615 \text{ mL/m}^2$ ). Biliary leakage developed in three patients, which was managed successfully by additional percutaneous drain placement or postoperative drain change. There were no cases of PHLF or mortality in the PVTT(+) group.

### Comparison of surgical outcomes with other hepatectomy indications using the ICG test

The safety limit of hepatectomy for HCC patients is based on three criteria: the presence or absence of ascites, the total bilirubin level, and the ICG-R15; collectively named the “Makuuchi criteria.” The absolute value of these criteria is supported by studies showing no mortality in > 1000 cases in 2003 [23, 24]. In the present series, the condition of 6 of the 12 patients (Nos. 2, 5, 6, 7, 8, and 9) was beyond these criteria; however, there was no PHLF and no mortality (Table 3).

The ICG-Krem is also a standard used for hepatectomy indications, and an ICG-Krem value of > 0.05 indicates a safe range for preventing PHLF [17]. In the present series, 2 of the 12 patients (Nos. 5 and 8) did not meet the criteria; however, there was also no mortality and no PHLF recorded for these patients (Table 3). We assessed the relationship between fFRLV and ICG-Krem, and the two values exhibited a relationship ( $r^2=0.387$ ,  $p=0.037$ ) (Supplemental Fig. 1a). ICG-Krem was not correlated with any major complications ( $p=0.086$ ) or with the length of hospital stay after surgery ( $p=0.119$ ).

### Comparison of surgical outcomes with functional %RLV using the 3D-CT/SPECT fusion imaging method

Table 2 shows the results of functional %RLV using the 3D-CT/SPECT imaging method. The results of %RLV using the 3D-CT/SPECT fusion method also reflected decreased regional liver function by PVTT; hence, the functional %RLV was higher than the %RLV in most patients, although in two patients (Nos. 1 and 9), the functional %RLV was lower than the %RLV and increases in functional %RLV compared with %RLV were less than 5% in three patients (Nos. 6, 10 and 11).

Assessment using 3D-CT/SPECT could not identify a relationship between fFRLV and functional %RLV ( $r^2=0.271$ ,  $p=0.083$ ; Supplemental Fig. 1b). Since none of the patients with PVTT had PLFH, we also

**Table 2** Characteristics of the hepatocellular carcinoma patients with portal vein tumor thrombus

Patient no.	Age (years)	Sex	Liver background	Tumor diameter (cm)	Vp	ICG-R15 (%)	ICG-Krem	%RLV (%)	Functional %RLV of 3D-CT/SPECT fusion (%)	fFRLV (ml/m <sup>2</sup> )	Procedure
1	67	F	HCV	7.8	2	8.6	0.076	46.1	41.9	709	Right hepatectomy
2	77	M	HCV	8	3	28.5	0.064	76.5	87.9	972	Left hepatectomy
3	73	M	HCV	1.3	3	13.3	0.104	77.3	86	1242	Extended left hepatectomy
4	60	M	HCV	3.5	2	15.3	0.087	69.6	79.8	1137	Left hepatectomy
5	77	M	HCV	4	3	26.7	0.049	56.1	63.1	486	Left hepatectomy
6	65	M	NBNC	7.2	2	26.3	0.070	79.1	80.7	964	Posterior sectionectomy
7	71	M	HBV	5	4	20.3	0.057	53.3	63.9	682	Right hepatectomy
8	71	F	NBNC	11.6	2	36.2	0.046	68	82.6	659	Left hepatectomy
9	70	M	NBNC	3.7	3	21.4	0.067	65.4	54.5	612	Extended left hepatectomy
10	70	M	NBNC	10.7	4	13.4	0.106	79.1	82.5	761	Left hepatectomy
11	65	M	HCV	3	3	16.4	0.081	67	70.8	1201	Extended left hepatectomy
12	78	M	NBNC	11.7	3	22.1	0.068	67.6	80.8	838	Right hepatectomy

HCC hepatocellular carcinoma, *PVTT* portal vein tumor thrombus, *BMI* body mass index, *ICG-R15* indocyanine green retention rate at 15 min, *ICG-Krem* ICG-K of the remnant liver volume, %RLV percentage of remnant liver volume, *3D-CT* three-dimensional computed tomography, *SPECT* single photon emission computed tomography, *fFRLV* functional future remnant liver volume, *HCV* hepatitis C virus, *NBNC* non-B non-C liver dysfunction, *HBV* hepatitis B virus

**Table 3** Surgical outcomes of the hepatocellular carcinoma patients with portal vein tumor thrombus

Patient no.	Procedure	Operative time (min)	Blood loss (mL)	Blood transfusion	Postoperative complication	PHLF	Length of hospital stay (days)
1	Right hepatectomy	542	1001	+	–	–	19
2	Left hepatectomy	499	194	–	–	–	12
3	Extended left hepatectomy	462	392	–	–	–	12
4	Left hepatectomy	595	295	–	–	–	10
5	Left hepatectomy	682	2368	+	–	–	14
6	Posterior sectionectomy	504	180	–	–	–	10
7	Right hepatectomy	411	190	–	Bile leak	–	23
8	Left hepatectomy	323	383	+	Bile leak	–	37
9	Extended left hepatectomy	345	61	–	Bile leak	–	24
10	Left hepatectomy	320	568	–	–	–	17
11	Extended left hepatectomy	477	285	–	–	–	21
12	Right hepatectomy	394	450	–	–	–	19

HCC hepatocellular carcinoma, PVTT portal vein tumor thrombus, PHLF post-hepatectomy liver failure

evaluated these two imaging values compared with other surgical outcomes such as major complication and length of hospital stay. The fFRLV and %RLV using 3D-CT/SPECT fusion had no correlation with the occurrence of major complications ( $p=0.086$  and  $p=0.578$ , respectively). The fFRLV was significantly related to the length of hospital stay after surgery ( $p=0.036$ ) but 3D-CT/SPECT fusion had no correlation ( $p=0.584$ ).

### MRI of the area occluded by PVTT and difference in the LMR between the occluded and non-occluded area

The T1 images of EOB-MRI, 20 min after EOB injection, revealed that the SI of the area occluded by PVTT was lower than that of the non-occluded area, which represents the remnant liver after hepatic resection (Fig. 1b–d). The value of LMR in the occluded area was lower in most patients (Fig. 1b). The difference in LMR values was assessed between the area occluded with PVTT and the non-occluded area (Fig. 3). The LMR of the occluded area was significantly lower than that of the non-occluded area ( $p=0.004$ ), suggesting decreased liver function with occlusion by PVTT.

### Correlations between ICG-R15 and LMR and between ICG-R15 and fFRLV

We assessed the correlations between ICG-R15 and LMR and between ICG-R15 and fFRLV, to examine the whole-liver function and regional liver function in each group. ICG-R15 and LMR tended to have a slight correlation in the PVTT(–) group ( $r=-0.430$ ,  $p=0.001$ ) (Fig. 4a). However, ICG-R15 and LMR were not correlated in the PVTT(+)

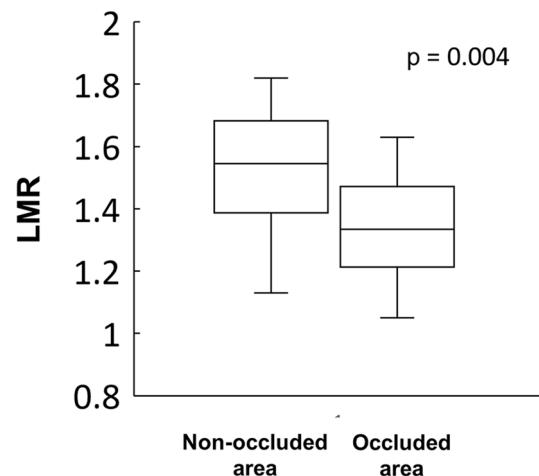


**Fig. 3** Functional liver scores (LMR, liver-to-muscle ratio) in the area occluded by portal vein tumor thrombus vs. the non-occluded area. The LMR of the occluded area was significantly lower than that of the non-occluded area ( $p=0.004$ ), indicating decreased liver function in the presence of occlusion

group ( $r=-0.204$ ,  $p=0.504$ ) (Fig. 4c). The fFRLV values were not correlated with ICG-R15 in either group (Fig. 4b, d).

### Discussion

The current study demonstrated that fFRLV, assessed using EOB-MRI, can help to establish the operative indications for HCC in patients with PVTT. Typically, the indication for hepatic resection is based on whole-liver function parameters, such as ICG-R15 or Child–Pugh scores, and volume



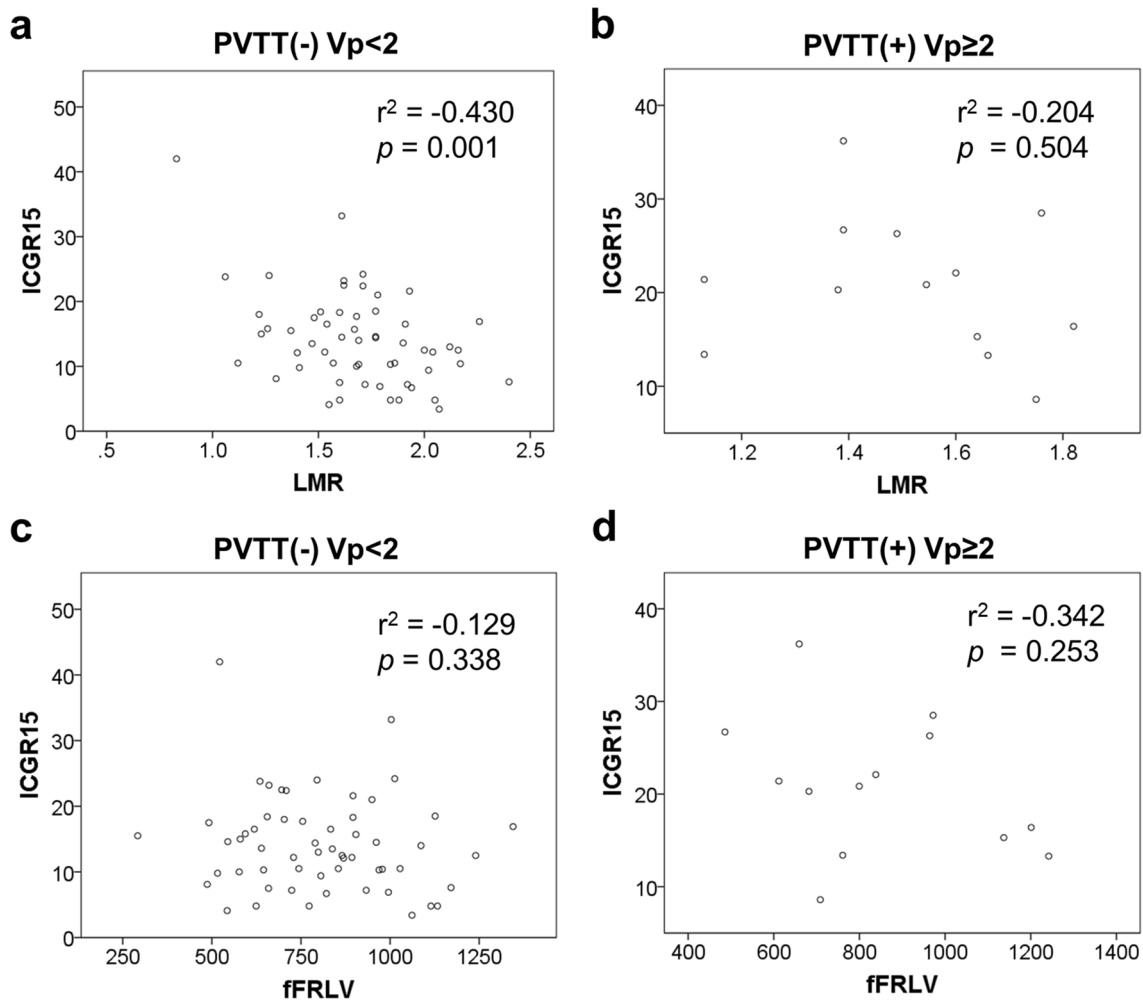


**Fig. 4** Correlation scatter plots between the indocyanine green retention rate at 15 min (ICG-15R) and the liver-to-muscle ratio (LMR) and between the ICG-15R and functional future remnant liver volume (fFRLV) in each group. **a** Correlation of ICG-15R and LMR in the

portal vein tumor thrombus-negative [PVTT(-)] group. **b** Correlation of ICG-15R and fFRLV in the PVTT(-) group. **c** Correlation of ICG-15R and LMR in the PVTT(+) group. **d** Correlation of ICG-15R and fFRLV in the PVTT(+) group

analysis to ensure adequate future remnant liver to prevent PHLF [18, 25, 26]. Surgeons can evaluate the regional liver functional volume easily, using imaging analysis methods of determining surgical indication. We reported previously that fFRLV was a good predictor of postoperative liver-related morbidity and PHLF after hepatectomy [11, 12]. To our knowledge, this is the first study to evaluate the significance of fFRLV assessed using EOB-MRI in HCC patients with PVTT.

Previous studies have suggested that EOB-MRI can be used to estimate liver function [8–10], and LMR is one of the quantitative indicators of liver function per unit liver volume [8]. Galactosyl human serum albumin (GSA) measurement is another method of quantitative liver function assessment [27]. Recently, the technetium (Tc)-99 m-GSA scintigraphy/SPECT and CT fusion system was described as a novel method that enables simultaneous evaluation of

the volume of any part of the liver and the regional liver functional reserve [28]. EOB-MRI has been reported as a better modality than Tc-99 m-GSA-SPECT due to the spatial resolution of EOB-MRI being superior, enabling the detailed assessment of regional liver function concomitantly with the diagnosis of hepatic lesions [29]. A previous study that investigated the accuracy of functional liver volume estimation using EOB-MRI compared with that using Tc-99 m-SPECT and CT fusion imaging, concluded that Tc-99 m-GSA-SPECT tended to underestimate the function of the left lobe and to overestimate the function of the right lobe [30]. This study suggested that functional %RLV using the 3D-CT/SPECT fusion method is a good reflection of the area occluded by PVTT. However, two cases were negative and three had small increases of liver function in the area not occluded by PVTT. Moreover, functional %RLV using 3D-CT/SPECT was not related to surgical outcomes.

Therefore, EOB-MRI could be a useful method for estimating the true regional functional liver reserve.

We also compared surgical outcomes between fFRLV and ICG-Krem. ICG-Krem was a good predictor, since 10 of the 12 PVTT(+) group patients met the criteria and only 2 did not. Although the ICG-K value is reflected as total liver function, ICG-Krem contains the element that predicts future remnant liver volume as %RLV. Therefore, ICG-Krem might be as good a predictor as fFRLV using EOB-MRI. However, our PVTT(+) group was relatively small, and it is difficult to evaluate the superiority of fFRLV over ICG-Krem. These two criteria in terms of hepatectomy indications should be compared in a prospective study with a larger population.

In this study, the LMR of the occluded area was significantly lower than that of the non-occluded area, which suggests decreased regional liver functional reserve in the presence of occlusion by PVTT. Empirically, we would expect the area occluded by PVTT to have reduced liver function; however, no method for evaluating the regional liver functional reserve of the occluded area has been reported. A method for evaluating the regional liver functional reserve may be more reliable than methods that evaluate the function of the whole liver. The advantage of this imaging technique for fFRLV assessment over Tc-99 m-single photon emission CT fusion imaging is that EOB-MRI is routinely performed preoperatively in the clinical setting to diagnose liver lesions. Moreover, ICG-R15 and LMR tended to show a correlation in the PVTT(−) group, but not in the PVTT(+) group. These results indicate that ICG-R15, as a whole-liver functional test, could not accurately evaluate the regional function of the remnant liver as it may reflect the area occluded by PVTT as a “false positive value.” LMR is better for evaluating regional liver function, especially in patients with PVTT. The fFRLV is calculated by multiplying the LMR and the remnant volume and thus, appears to not correlate with ICG-R15 in either group. We believe that measuring fFRLV along with LMR could be one of the most reliable methods for evaluating the regional liver functional reserve and for precisely determining the operative indication in HCC patients with PVTT.

The current study showed that both LMR and fibrosis markers such as M2BPGi and VTQ were significantly more increased in the PVTT(+) group than in the PVTT(−) group. LMR could be correlated, not only with liver function, but also with liver fibrosis in HCC patients. As the value of fFRLV is calculated by multiplying LMR and RLV, fFRLV represents both regional liver function and liver volume. Accordingly, fFRLV measurement is a more reliable method for predicting PHLF than whole-liver functional blood tests or volumetric analysis only.

Although fFRLV could precisely predict PHLF in HCC patients with PVTT, operative procedures should still be

performed cautiously in these patients. In this series, the rate of postoperative major complications tended to be higher in the PVTT(+) group. The values of VTQ and M2BPGi in patients with PVTT indicated severe liver fibrosis and low functional reserve in the remnant liver. Therefore, surgery is potentially riskier in patients with PVTT. Even if PHLF could be prevented through the preoperative evaluation of fFRLV, surgeons should still perform hepatectomy with great care in patients with PVTT to optimize a safe postoperative course.

The limitations of this study were that it was retrospective, the sample size was small and the number of events was limited. Multicenter prospective studies are needed to evaluate the usefulness of fFRLV assessed using EOB-MRI for HCC patients with PVTT, as well as to evaluate whether fFRLV could be used as a precise determinant of operative indication in these patients.

In conclusion, assessing fFRLV by EOB-MRI could be a useful tool for estimating the regional functional liver reserve in HCC patients with PVTT. This method could allow more precise determination of the operative indication to prevent liver-related morbidity or PHLF in patients undergoing hepatectomy.

**Acknowledgments** We thank H. Tanaka, K. Hagiwara, K. Hoshino, and R. Muranushi for collecting data that formed the basis of this study. We also thank K. Ujita and J. Fukuda for their special assistance in image analysis.

**Funding** This research did not receive any specific grant from funding agencies in the public, commercial, or not-for-profit sectors.

## Compliance with ethical standards

**Conflict of interest** We have no conflicts of interest to declare.

## References

1. Forner A, Llovet JM, Bruix J. Hepatocellular carcinoma. *Lancet*. 2012;379:1245–55. [https://doi.org/10.1016/s0140-6736\(11\)61347-0](https://doi.org/10.1016/s0140-6736(11)61347-0).
2. Llovet JM, Bustamante J, Castells A, Vilana R, Ayuso Mdel C, Sala M, et al. Natural history of untreated nonsurgical hepatocellular carcinoma: rationale for the design and evaluation of therapeutic trials. *Hepatology*. 1999;29:62–7. <https://doi.org/10.1002/hep.510290145>.
3. Ikai I, Hatano E, Hasegawa S, Fujii H, Taura K, Uyama N, et al. Prognostic index for patients with hepatocellular carcinoma combined with tumor thrombosis in the major portal vein. *J Am Coll Surg*. 2006;202:431–8. <https://doi.org/10.1016/j.jamcollsur.2005.11.012>.
4. Ban D, Shimada K, Yamamoto Y, Nara S, Esaki M, Sakamoto Y, et al. Efficacy of a hepatectomy and a tumor thrombectomy for hepatocellular carcinoma with tumor thrombus extending to the main portal vein. *J Gastrointest Surg*. 2009;13:1921–8. <https://doi.org/10.1007/s11605-009-0998-0>.

5. Matono R, Yoshiya S, Motomura T, Toshima T, Kayashima H, Masuda T, et al. Factors linked to longterm survival of patients with hepatocellular carcinoma accompanied by tumour thrombus in the major portal vein after surgical resection. *HPB (Oxford)*. 2012;14:247–53. <https://doi.org/10.1111/j.1477-2574.2011.00436.x>.
6. Shi J, Lai EC, Li N, Guo WX, Xue J, Lau WY, et al. Surgical treatment of hepatocellular carcinoma with portal vein tumor thrombus. *Ann Surg Oncol*. 2010;17:2073–80. <https://doi.org/10.1245/s10434-010-0940-4>.
7. Ye JZ, Wang YY, Bai T, Chen J, Xiang BD, Wu FX, et al. Surgical resection for hepatocellular carcinoma with portal vein tumor thrombus in the Asia-Pacific region beyond the Barcelona Clinic Liver Cancer treatment algorithms: a review and update. *Oncotarget*. 2017;8:93258–78. <https://doi.org/10.18632/oncotarget.18735>.
8. Nishie A, Ushijima Y, Tajima T, Asayama Y, Ishigami K, Kakihara D, et al. Quantitative analysis of liver function using superparamagnetic iron oxide- and Gd-EOB-DTPA-enhanced MRI: comparison with Technetium-99 m galactosyl serum albumin scintigraphy. *Eur J Radiol*. 2012;81:1100–4. <https://doi.org/10.1016/j.ejrad.2011.02.053>.
9. Tajima T, Takao H, Akai H, Kiryu S, Imamura H, Watanabe Y, et al. Relationship between liver function and liver signal intensity in hepatobiliary phase of gadolinium ethoxybenzyl diethylenetriamine pentaacetic acid-enhanced magnetic resonance imaging. *J Comput Assist Tomogr*. 2010;34:362–6. <https://doi.org/10.1097/RCT.0b013e3181cd3304>.
10. Yamada A, Hara T, Li F, Fujinaga Y, Ueda K, Kadoya M, et al. Quantitative evaluation of liver function with use of gadoxetate disodium-enhanced MR imaging. *Radiology*. 2011;260:727–33. <https://doi.org/10.1148/radiol.11100586>.
11. Itoh S, Yoshizumi T, Shirabe K, Kimura K, Okabe H, Harimoto N, et al. Functional remnant liver assessment predicts liver-related morbidity after hepatic resection in patients with hepatocellular carcinoma. *Hepatol Res*. 2017;47:398–404. <https://doi.org/10.1111/hepr.12761>.
12. Araki K, Harimoto N, Kubo N, Watanabe A, Igarashi T, Tsukagoshi M, et al. Functional remnant liver volumetry using Gd-EOB-DTPA-enhanced magnetic resonance imaging (MRI) predicts post-hepatectomy liver failure in resection of more than one segment. *HPB (Oxford)*. 2020;22:318–27. <https://doi.org/10.1016/j.hpb.2019.08.002>.
13. Dindo D, Demartines N, Clavien PA. Classification of surgical complications: a new proposal with evaluation in a cohort of 6336 patients and results of a survey. *Ann Surg*. 2004;240:205–13.
14. Rahbari NN, Garden OJ, Padbury R, Brooke-Smith M, Crawford M, Adam R, et al. Posthepatectomy liver failure: a definition and grading by the International Study Group of Liver Surgery (ISGLS). *Surgery*. 2011;149:713–24. <https://doi.org/10.1016/j.surg.2010.10.001>.
15. Nishie A, Asayama Y, Ishigami K, Tajima T, Kakihara D, Nakayama T, et al. MR prediction of liver fibrosis using a liver-specific contrast agent: superparamagnetic iron oxide versus Gd-EOB-DTPA. *J Magn Reson Imaging*. 2012;36:664–71. <https://doi.org/10.1002/jmri.23691>.
16. Ninomiya M, Shirabe K, Kayashima H, Ikegami T, Nishie A, Harimoto N, et al. Functional assessment of the liver with gadolinium-ethoxybenzyl-diethylenetriamine penta-acetate-enhanced MRI in living-donor liver transplantation. *Br J Surg*. 2015;102:944–51. <https://doi.org/10.1002/bjs.9820>.
17. Nagino M, Kamiya J, Nishio H, Ebata T, Arai T, Nimura Y. Two hundred forty consecutive portal vein embolizations before extended hepatectomy for biliary cancer: surgical outcome and long-term follow-up. *Ann Surg*. 2006;243:364–72. <https://doi.org/10.1097/01.sla.0000201482.11876.14>.
18. Shirabe K, Shimada M, Gion T, Hasegawa H, Takenaka K, Utsunomiya T, et al. Postoperative liver failure after major hepatic resection for hepatocellular carcinoma in the modern era with special reference to remnant liver volume. *J Am Coll Surg*. 1999;188:304–9.
19. Jones RM, Moulton CE, Hardy KJ. Central venous pressure and its effect on blood loss during liver resection. *Br J Surg*. 1998;85:1058–60. <https://doi.org/10.1046/j.1365-2168.1998.00795.x>.
20. Iguchi T, Ikegami T, Fujiyoshi T, Yoshizumi T, Shirabe K, Maehara Y. Low positive airway pressure without positive end-expiratory pressure decreases blood loss during hepatectomy in living liver donors. *Dig Surg*. 2017;34:192–6. <https://doi.org/10.1159/000447755>.
21. Otsubo T, Takasaki K, Yamamoto M, Katsuragawa H, Katagiri S, Yoshitoshi K, et al. Bleeding during hepatectomy can be reduced by clamping the inferior vena cava below the liver. *Surgery*. 2004;135:67–73. <https://doi.org/10.1016/s0039>.
22. Rahbari NN, Koch M, Zimmermann JB, Elbers H, Bruckner T, Contin P, et al. Intrahepatic inferior vena cava clamping for reduction of central venous pressure and blood loss during hepatic resection: a randomized controlled trial. *Ann Surg*. 2011;253:1102–10. <https://doi.org/10.1097/SLA.0b013e318214bee5>.
23. Miyagawa S, Makuuchi M, Kawasaki S, Kakazu T. Criteria for safe hepatic resection. *Am J Surg*. 1995;169:589–94.
24. Imamura H, Seyama Y, Kokudo N, Maema A, Sugawara Y, Sano K, et al. One thousand fifty-six hepatectomies without mortality in 8 years. *Arch Surg*. 2003;138:1198–206. <https://doi.org/10.1001/archsurg.138.11.1198> (discussion 206).
25. Kubota K, Makuuchi M, Kusaka K, Kobayashi T, Miki K, Hasegawa K, et al. Measurement of liver volume and hepatic functional reserve as a guide to decision-making in resectional surgery for hepatic tumors. *Hepatology*. 1997;26:1176–81. <https://doi.org/10.1053/jhep.1997.v26.pm0009362359>.
26. Shoup M, Gonen M, D'Angelica M, Jarnagin WR, DeMatteo RP, Schwartz LH, et al. Volumetric analysis predicts hepatic dysfunction in patients undergoing major liver resection. *J Gastrointest Surg*. 2003;7:325–30.
27. Kwon AH, Ha-Kawa SK, Uetsuji S, Inoue T, Matsui Y, Kamiyama Y. Preoperative determination of the surgical procedure for hepatectomy using technetium-99 m-galactosyl human serum albumin (99 mTc-GSA) liver scintigraphy. *Hepatology*. 1997;25:426–9. <https://doi.org/10.1002/hep.510250228>.
28. Hayashi H, Beppu T, Okabe H, Kuroki H, Nakagawa S, Imai K, et al. Functional assessment versus conventional volumetric assessment in the prediction of operative outcomes after major hepatectomy. *Surgery*. 2015;157:20–6. <https://doi.org/10.1016/j.surg.2014.06.013>.
29. Utsunomiya T, Shimada M, Hanaoka J, Kanamoto M, Ikemoto T, Morine Y, et al. Possible utility of MRI using Gd-EOB-DTPA for estimating liver functional reserve. *J Gastroenterol*. 2012;47:470–6. <https://doi.org/10.1007/s00535-011-0513-8>.
30. Morine Y, Enkhbold C, Imura S, Ikemoto T, Iwahashi S, Saito YU, et al. Accurate estimation of functional liver volume using Gd-EOB-DTPA MRI compared to MDCT/(99m)Tc-SPECT fusion imaging. *Anticancer Res*. 2017;37:5693–700. <https://doi.org/10.21873/anticancer.12006>.

**Publisher's Note** Springer Nature remains neutral with regard to jurisdictional claims in published maps and institutional affiliations.